JET ENGINE'S ROTATION SPEED CONTROL BASED ON THE FUEL'S INJECTION DIFFERENTIAL PRESSURE'S CONTROL

Alexandru Nicolae TUDOSIE

University of Craiova, Faculty of Electrical Engineering, Avionics Department,
e-mail: atudosie@elth.ucv.ro, antudosie@yahoo.com

Abstract **– This paper deals with an automatic system for a jet engine's speed control, which uses a differential pressure controller coupled with the engine's fuel pump. One has established the system's non-linear mathematical model, the linearised and the non-dimensional mathematical model; based on this model, the block-diagram with transfer functions and the system's transfer function were issued. A stability study was performed, which has determined the system's stability domains; system's quality was also studied (some simulations were performed), based on its step response, considering the throttle's position as input and the engine's speed as output, for the maximum engine's operating regime. The co-efficient ensemble was determined for a single-spool jet engine RD9- type.**

Keywords: *jet engine, speed, fuel, pressure, control, actuator, slide valve, throttle.*

1. INTRODUCTION

For an aircraft gas-turbine engine, particularly for a jet engine, the speed n control is one of the most important issues, both for various flight speeds and flight altitudes, and it's currently realized using specific hydro-mechanical and/or electro-mechanical controllers. This paper deals with such a controller, which assures a constant value of the dosage valve's differential pressure, the fuel flow rate amount Q_i being determined by the dosage valve's opening.

As figure 1 show, a rotation speed control system consists of four main parts: I-fuel pump with plungers (4) and mobile plate (5); II-pump's actuator with spring (22), piston (23) and rod (6); III-differential pressure sensor with slide valve (17), preset bolt (20) and spring (18); IV-dosage valve,

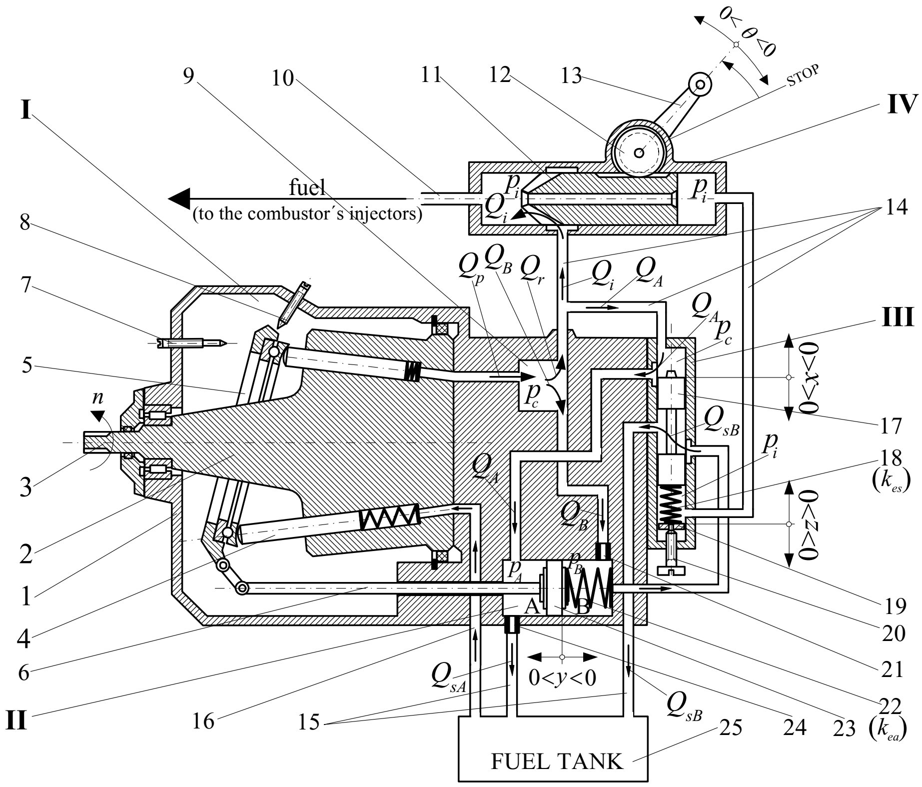

Figure 1: Engine's speed control system's functional diagram

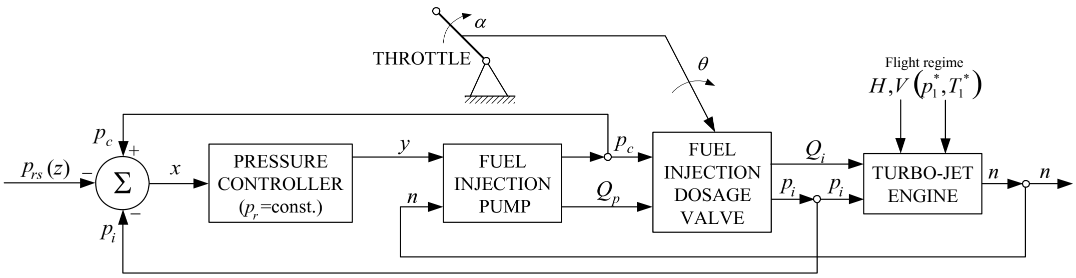

Figure 2: System's functional diagram

with its slide valve (11), connected to the engine's throttle through the rocking lever (13).

The system operates by keeping a constant difference of pressure, between the pump's pressure chamber (9) and the injectors' pipe (10), equal to the preset value (proportional to the spring (18) pre-compression, set by the adjuster bolt (20)). The engine's necessary fuel flow rate Q_i and, consequently, the engine's speed *n*, is controlled by the co-relation between the $p_r = p_c - p_i$ differential pressure's amount and the dosage valve's variable slot opening (proportional to the (13) rocking lever's angular displacement θ).

A functional block diagram of the system is presented in figure 2.

2. SYSTEM'S MATHEMATICAL MODEL

2.1. System's motion non-linear equations

The non-linear mathematical model consists of the motion equations for each above described sub-system, as follows:

a) fuel pump flow rate's equations

$$Q_p = Q_p(n, y)\,, \tag{1}$$

$$Q_p = Q_A + Q_B + Q_i\,, \tag{2}$$

b) pressure sensor's equations

$$Q_A = \mu_s b_s (x_s + x)\sqrt{2\rho^{-1}}\sqrt{p_c - p_A}\,, \tag{3}$$

$$Q_B = \mu_d \frac{\pi d_d^2}{4}\sqrt{2\rho^{-1}}\sqrt{p_c - p_B}\,, \tag{4}$$

$$S_{sv}\left(p_c - p_i\right) = m_s \frac{\mathrm{d}^2 x}{\mathrm{d}t^2} + \xi \frac{\mathrm{d}x}{\mathrm{d}t} + k_{es}(z + x_s + x)\,, \tag{5}$$

c) fuel pump's actuator's equations

$$Q_A - Q_{sA} = \beta V_{A0}\frac{\mathrm{d}p_A}{\mathrm{d}t} - S_A \frac{\mathrm{d}y}{\mathrm{d}t}\,, \tag{6}$$

$$Q_B - Q_{sB} = \beta V_{B0}\frac{\mathrm{d}p_B}{\mathrm{d}t} + S_B \frac{\mathrm{d}y}{\mathrm{d}t}\,, \tag{7}$$

$$Q_{sA} = \mu_d \frac{\pi d_d^2}{4}\sqrt{2\rho^{-1}}\sqrt{p_A - p_s}\,, \tag{8}$$

$$Q_{sB} = \mu_s b_s (x_s + x)\sqrt{2\rho^{-1}}\sqrt{p_c - p_B}\,, \tag{9}$$

$$S_B p_B - S_A p_A = m_p \frac{\mathrm{d}^2 y}{\mathrm{d}t^2} + \xi \frac{\mathrm{d}y}{\mathrm{d}t} + k_{ea}(y_s + y)\,, \tag{10}$$

d) dosage valve's equation

$$Q_i = \mu_i b_i r_{dw} \frac{\theta - \theta_s}{\pi}\sqrt{2\rho^{-1}}\sqrt{p_c - p_i}\,, \tag{11}$$

e) jet engine's equation (for the rotation speed *n*)

$$n = n\left(Q_i, p_1^*, T_1^*\right), \tag{12}$$

where $Q_p, Q_i, Q_A, Q_B, Q_{sA}, Q_{sB}$ are fuel flow rates, p_c - pump's chamber's pressure, p_i -fuel's injection pressure, p_A - actuator's A chamber's pressure, p_B - actuator's B chamber's pressure, p_s -low pressure's circuit's pressure, μ_d , μ_s , μ_i -flow rate co-efficient, d_d - (21) and (24) drossels' diameters, S_A, S_B - piston's surfaces, $S_A \approx S_B$, S_{sv} -slide valve's frontal surface, b_s -sensor's slide valve's slot width, b_i - dosage valve's slide valve's slot width, k_{ea}, k_{es} -spring elastic constants, V_{A0} -actuator's active A chamber's volume, V_{B0} -actuator's active B chamber's volume, β -fuel's compressibility co-efficient, ρ -fuel's density, ξ -viscous friction co-efficient, m_p-actuator's mobile ensemble's mass, m_s-pressure sensor's mobile slide valve's mass, θ -dosing valve's lever's angular displacement (which is proportional to the throttle's displacement α), r_{dw} - (12) driving wheel's radius, *x*-sensor's slide valve's displacement, *z*-sensor's spring preset, *y*-actuator's rod's displacement, p_1^*, T_1^* -jet engine's inlet's gas-dynamic parameters (total pressure and total temperature).

So, the above described 12 non-linear motion equations are building the system's non-linear mathematical model.

2.2 Linear mathematical model

Assuming the small-disturbances hypothesis, one can obtain a linear form of the model; so, assuming that each *X* parameter can be expressed as

$$X = X_0 + \frac{\Delta X}{1} + \frac{(\Delta X)^2}{2} + \ldots + \frac{(\Delta X)^n}{n}, \quad (13)$$

(where X_0 is the steady state regime's *X*-value and ΔX -deviation or static error) and, neglecting the terms which contains $(\Delta X)^r, r \geq 2$, one obtains a new form of the equation system (2)…(11), particularly in the neighborhood of a steady state operating regime, as follows:

$$\Delta Q_p = \Delta Q_A + \Delta Q_B + \Delta Q_i, \quad (14)$$

$$\Delta Q_A = k_{Ax}\Delta x + k_{Ac}(\Delta p_C - \Delta p_A), \quad (15)$$

$$\Delta Q_{sA} = k_{sAA}\Delta p_A, \quad (16)$$

$$\Delta Q_B = k_{Bc}(\Delta p_C - \Delta p_B), \quad (17)$$

$$\Delta Q_{sB} = k_{Bx}\Delta x + k_{sBB}\Delta p_B, \quad (18)$$

$$\Delta Q_i = k_{i\theta}\Delta\theta + k_{ic}(\Delta p_C - \Delta p_i), \quad (19)$$

$$k_{Ax}\Delta x + k_{Ac}(\Delta p_C - \Delta p_A) - k_{sAA}\Delta p_A = \beta V_{A0}\frac{\mathrm{d}}{\mathrm{d}t}\Delta p_A - S_A\frac{\mathrm{d}}{\mathrm{d}t}\Delta y, \quad (20)$$

$$-k_{Bx}\Delta x + k_{Bc}(\Delta p_C - \Delta p_B) - k_{sBB}\Delta p_B = \beta V_{B0}\frac{\mathrm{d}}{\mathrm{d}t}\Delta p_B + S_B\frac{\mathrm{d}}{\mathrm{d}t}\Delta y, \quad (21)$$

$$S_{sv}(\Delta p_C - \Delta p_i) = m_s\frac{\mathrm{d}^2}{\mathrm{d}t^2}\Delta x + \xi\frac{\mathrm{d}}{\mathrm{d}t}\Delta x + k_{es}(\Delta z + \Delta x) \quad (22)$$

$$S_B\Delta p_B - S_A\Delta p_A = m_p\frac{\mathrm{d}^2}{\mathrm{d}t^2}\Delta y + \xi\frac{\mathrm{d}}{\mathrm{d}t}\Delta y + k_{ea}\Delta y. \quad (23)$$

In the above equations one has used the annotations

$$k_{Ax} = \mu_s b_s\sqrt{2\rho^{-1}}\sqrt{p_{C0} - p_{A0}}, k_{AC} = \mu_s b_s\frac{(x_s + x_0)\sqrt{2\rho^{-1}}}{\sqrt{p_{C0} - p_{A0}}},$$

$$k_{sAA} = \mu_d\frac{\pi d_d^2}{4}\frac{\sqrt{2\rho^{-1}}}{2\sqrt{p_{A0}}}, k_{BC} = \mu_d\frac{\pi d_d^2}{8}\frac{\sqrt{2\rho^{-1}}}{\sqrt{p_{C0} - p_{B0}}},$$

$$k_{Bx} = \mu_s b_s\sqrt{2\rho^{-1}}\sqrt{p_{B0}}, k_{sBB} = \mu_s b_s\frac{(x_s + x_0)\sqrt{2\rho^{-1}}}{\sqrt{p_{B0}}},$$

$$k_{i\theta} = \frac{\mu_i b_i r_{12}}{\pi}\sqrt{2\rho^{-1}}\sqrt{p_{C0} - p_{i0}},$$

$$k_{ic} = \frac{\mu_i b_i r_{12}}{\pi}\frac{(\theta_0 - \theta_s)\sqrt{2\rho^{-1}}}{2\sqrt{p_{C0} - p_{i0}}}. \quad (24)$$

For a steady state regime, the fuel flow rates through the drossels and the sensor's slots are equal, $Q_{A0} = Q_{sA0}$ and $Q_{B0} = Q_{sB0}$; meanwhile, the pressure values in the actuator's chambers must satisfy the balance equation

$$p_{A0} = p_{B0} + \frac{k_{ea}}{S_A}y_0, \quad (25)$$

respectively in the sensor's chambers

$$p_{i0} = p_{C0} + \frac{k_{es}}{S_{sv}}(z_0 + x_0). \quad (26)$$

The equations (24) and (25) are giving the pressures expressions for the steady state regime, as follows

$$p_{C0} = \frac{k_{ea}}{S_A}y_0\frac{\gamma + 1}{\gamma - 1}, \quad (27)$$

$$p_{A0} = \frac{k_{ea}}{S_A}y_0\frac{\gamma}{\gamma - 1}, \quad (28)$$

$$p_{B0} = \frac{k_{ea}}{S_A}y_0\frac{1}{\gamma - 1}, \quad (29)$$

where $\gamma = \left(\frac{\mu_s}{\mu_d}\right)^2\frac{16b_s^2x_0^2}{\pi^2 d_d^4}$.

One chooses the geometry of the drossels (21 and 24), respectively of the sensor's slots, in order to satisfy the relation

$$d_d = 2\sqrt{b_s\frac{\mu_s}{\mu_d}\frac{(x_{\max} - x_{\min})}{\pi}}, \quad (30)$$

so that $k_{AC} \approx k_{BC}$. Assuming that the actuator's chambers' volumes, as well as the actuator's piston surfaces, could be considered as having very close values $(V_{A0} \approx V_{B0}, S_A \approx S_B)$ and adding the equation (20) to the multiplied by (-1) equation (21), one obtains

$$(k_{Ax} + k_{Bx})\Delta x + (k_{AC} + k_{sAA})(\Delta p_B - \Delta p_A) + \beta V_{A0}\frac{\mathrm{d}}{\mathrm{d}t}(\Delta p_B - \Delta p_A) = -2S_A\frac{\mathrm{d}}{\mathrm{d}t}\Delta y. \quad (31)$$

From the equations (14), (15), (17) and (19) it results

$$\Delta Q_p = k_{i\theta}\Delta\theta + k_{Ax}\Delta x + k_{ic}(\Delta p_C - \Delta p_i) + (k_{AC} + k_{BC})\Delta p_C - (k_{AC}\Delta p_A + k_{BC}\Delta p_B). \quad (32)$$

According to the above observations and assumptions, one obtains

$$(k_{AC} + k_{BC})\Delta p_C \approx (k_{AC}\Delta p_A + k_{BC}\Delta p_B), \quad (33)$$

so the equation (32) becomes

$$\Delta Q_p = k_{i\theta}\Delta\theta + k_{Ax}\Delta x + k_{ic}(\Delta p_C - \Delta p_i). \quad (32')$$

The equations (31), (32'), as well as the equations (19), (22) and (23), with the annotations (24), are building the system's linear mathematical model.

2.2. Non-dimensional mathematical model

Using the generic annotation $\overline{X} = \dfrac{\Delta X}{X_0}$, the above mathematical model can be transformed in a non-dimensional one. After applying, for each of the above mentioned equations, the Laplace transformer, one obtains the mathematical model's non-dimensional linearised form, as follows

$$k_{px}\overline{x} + (\tau_p \mathrm{s} + 1)(\overline{p_B} - \overline{p_A}) = -\tau_A \mathrm{s}\overline{y}, \tag{34}$$

$$\overline{p_B} - \overline{p_A} = k_{AB}(T_y^2 \mathrm{s}^2 + 2T_y \omega_0 \mathrm{s} + 1)\overline{y}, \tag{35}$$

$$\overline{p_C} - \overline{p_i} = k_{pic}(T_x^2 \mathrm{s}^2 + 2T_x \omega_0 \mathrm{s} + 1)\overline{x} + k_{iz}\overline{z}, \tag{36}$$

$$\overline{Q_p} = k_\theta \overline{\theta} + k_{Qx}\overline{x} + k_{Qp}(\overline{p_C} - \overline{p_i}), \tag{37}$$

$$\overline{Q_i} = k_\theta \overline{\theta} + k_{Qp}(\overline{p_C} - \overline{p_i}), \tag{38}$$

where the new system's co-efficient are

$$k_{px} = \frac{(k_{Ax} + k_{Bx})x_0}{(k_{AC} - k_{sAA})p_{C0}},\ \tau_p = \frac{\beta V_{A0}}{(k_{AC} - k_{sAA})p_{C0}},$$

$$\tau_p = \frac{2S_A y_0}{(k_{AC} - k_{sAA})p_{C0}},\ k_{AB} = \frac{k_{ea} y_0}{S_{sv} p_{C0}},\ T_y = \sqrt{\frac{m_p}{k_{ea}}},$$

$$2T_y\omega_0 = \frac{\xi}{k_{ea}},\ k_{pic} = \frac{k_{es}x_0}{S_{sv}p_0},\ k_{iz} = \frac{k_{es}z_0}{S_{sv}p_0},\ k_\theta = \frac{k_{i\theta}\theta_0}{Q_{p0}},$$

$$k_{Qx} = \frac{k_{Ax}x_0}{Q_{p0}},\ k_{Qp} = \frac{k_{ic}p_{C0}}{Q_{p0}},\ T_x = \sqrt{\frac{m_s}{k_{ea}}},\ 2T_x\omega_0 = \frac{\xi}{k_{es}}. \tag{39}$$

Adding the non-dimensional equation for the fuel pump and for the engine (engine's speed equation) [5,7]

$$\overline{Q_p} = k_{pn}\overline{n} + k_{py}\overline{y}, \tag{40}$$

$$(\tau_M \mathrm{s} + 1)\overline{n} = k_c \overline{Q_i} + k_{HV}\overline{p_1^*}, \tag{41}$$

one obtains the system's linear non-dimensional mathematical model, which is the source for the block diagram with transfer functions in figure 3.

For a constant flight regime, the term $k_{HV}\overline{p_1^*}$ in eq. (41) becomes null.

3. SYSTEM'S TRANSFER FUNCTION

The equations system (34)…(38), (40) and (41) can be simplified, keeping the same form in (39) for the co-efficient, if one assumes some plausible new hypothesis, such as: 1) the fuel's incompressibility $(\beta \approx 0)$, which means $\tau_A = 0$; 2) the viscous friction is very small $(\xi \approx 0)$, which means $2T_x\omega_0 = \dfrac{\xi}{k_{es}} = 0$ and $2T_y\omega_0 = \dfrac{\xi}{k_{ea}} = 0$; 3) small mass values (m_p, m_s) and, consequently, negligible inertial effects, which means $T_x = 0, T_y = 0$.

The new equation system is

$$(\tau_p \mathrm{s} + 1)(\overline{p_B} - \overline{p_A}) = -k_{px}\overline{x}, \tag{42}$$

$$\overline{p_B} - \overline{p_A} = k_{AB}\overline{y}, \tag{43}$$

$$\overline{x} = \frac{1}{k_{pic}}(\overline{p_C} - \overline{p_i}) - \frac{k_{iz}}{k_{pic}}\overline{z}, \tag{44}$$

$$\overline{p_C} - \overline{p_i} = \frac{1}{k_{Qp}}(\overline{Q_p} - k_\theta\overline{\theta} - k_{Qx}\overline{x}), \tag{45}$$

$$\overline{Q_i} = \overline{Q_p} - k_\theta\overline{\theta}, \tag{46}$$

$$\overline{Q_p} = k_{pn}\overline{n} + k_{py}\overline{y}, \tag{47}$$

$$(\tau_M \mathrm{s} + 1)\overline{n} = k_c\overline{Q_i}. \tag{48}$$

The simplified block diagram with transfer functions, based on the above model, is presented in figure 4.

The equations (42)…(48), after eliminating the intermediate arguments $\overline{p_A}, \overline{p_B}, \overline{p_C}, \overline{p_i}, \overline{Q_i}, \overline{Q_p}, \overline{y}, \overline{x}$, are

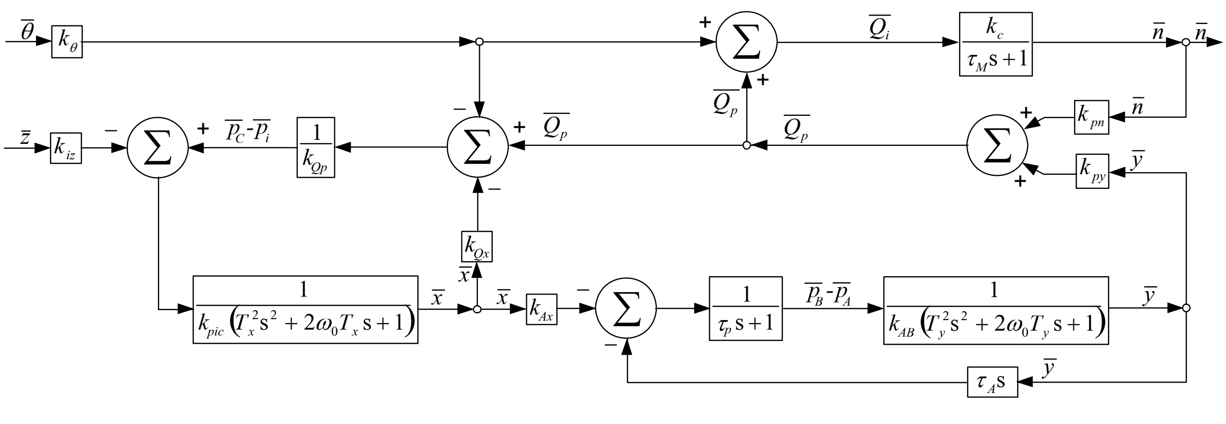

Figure 3: System's block diagram with transfer functions

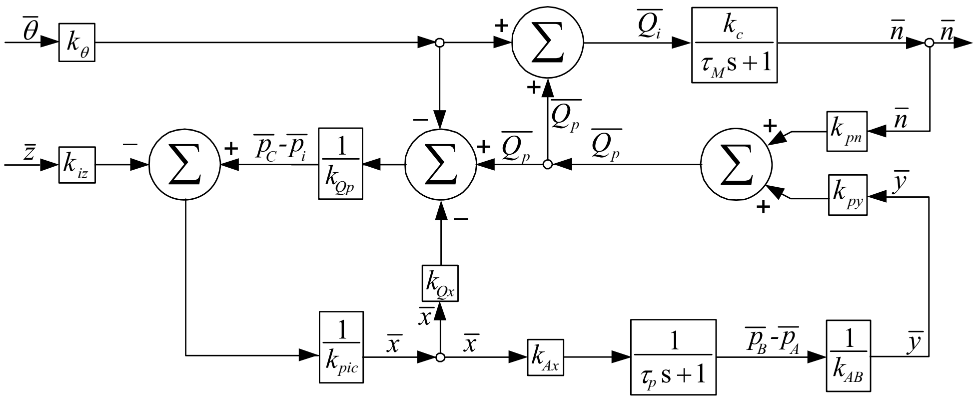

Figure 4: System's simplified block diagram with transfer functions

leading to an unique equation:

$$\left[\left(k_{pic}+k_{Qx}\right)\frac{k_{AB}}{k_{px}}\left(\tau_p s+1\right)\frac{\tau_M s+\left(1-k_c k_{pn}\right)}{k_c k_{py}}-\frac{\tau_M s+1}{k_c}\right]\overline{n}=$$

$$=k_{iz}\overline{z}+\left(k_{pic}+k_{Qx}\right)\frac{k_{AB}k_\theta}{k_{px}k_{py}}\left(\tau_p s+1\right)\overline{\theta}\,. \qquad (49)$$

System's transfer functions is $H_\theta(s)$, with respect to the dosage valve's rocking lever's position θ. A transfer function with respect to the setting z, $H_z(s)$, is not relevant, because the setting and adjustments are made during the pre-operational ground tests, not during the engine's current operation.
So, the main and the most important transfer function has the form below

$$H_\theta(s)=\frac{f_1 s+f_0}{g_2 s^2+g_1 s+g_0}\,, \qquad (50)$$

where the involved co-efficient are

$$f_1=k_c k_\theta \tau_p,\ f_0=k_c k_\theta,\ g_2=\tau_p\tau_M,$$

$$g_1=\tau_p\left(1-k_c k_{pn}\right)+\tau_M\left[1-\frac{k_{px}k_{py}}{k_{AB}\left(k_{pic}+k_{Qx}\right)}\right],$$

$$g_0=\left(1-k_c k_{pn}\right)-\frac{k_{px}k_{py}}{k_{AB}\left(k_{pic}+k_{Qx}\right)}\,. \qquad (51)$$

4. SYSTEM'S STABILITY

According to the system's transfer function form, the characteristic polynomial is a second degree one. So, in order to study the system's stability, one can use an algebraic criterion, Routh-Hurwitz, which imposes for stability that all the polynomial co-efficient must be strictly positive; so, that means that one obtains the inequalities:

$$\tau_p\tau_M>0\,, \qquad (52)$$

obviously, always realized, because both τ_y and τ_M are strictly positive quantities, being time constant of the actuator, respectively of the engine,

$$\tau_p\left(1-k_c k_{pn}\right)+\tau_M\left[1-\frac{k_{px}k_{py}}{k_{AB}\left(k_{pic}+k_{Qx}\right)}\right]>0\,, \qquad (53)$$

$$\left(1-k_c k_{pn}\right)-\frac{k_{px}k_{py}}{k_{AB}\left(k_{pic}+k_{Qx}\right)}>0\,. \qquad (54)$$

According to [5] and [7], the factor $1-k_c k_{pn}$ is a very important one, because its value is the one who gives information about the stability of the connection between the fuel pump and the jet engine's spool (rotor). For the actually operating engines, there are two cases involving it:

a) $0<k_c k_{pn}<1$, when the connection between the fuel pump and the spool is a stable object;
b) $k_c k_{pn}\geq 1$, when the connection between the fuel pump and the spool is an unstable object and it is compulsory to be assisted by a speed controller.

Each case will be studied separately.

Case a) $0<k_c k_{pn}<1$, so $1-k_c k_{pn}>0$

Replacing the co-efficient in (54) by their expressions, given by the annotation sets (24) and (39), one obtains

$$\frac{\mu_s b_s S_{sv}(\gamma+1)^2 y_0 Q_{p0}}{S_A(\gamma-1)^2 x_0\left(1-k_c k_{pn}\right)\left(\mu_s b_s\gamma x_0-\frac{\pi}{4}\mu_d d_d^2\sqrt{\gamma}\right)}k_{ea}-$$

$$-\mu_s b_s\sqrt{\frac{2y_0}{\rho S_A(\gamma-1)}}\sqrt{k_{ea}}+$$

$$+\frac{S_{sv}Q_{p0}(\gamma+1)^2}{(\gamma-1)\left(1-k_c k_{pn}\right)\left(\mu_s b_s\gamma x_0-\frac{\pi}{4}\mu_d d_d^2\sqrt{\gamma}\right)}<k_{es}\,, \qquad (55)$$

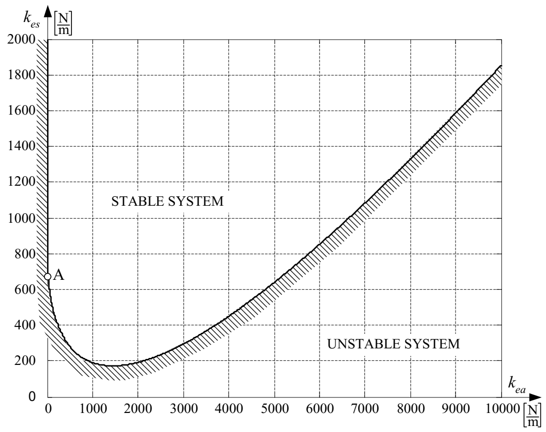

Figure 5: System's stability domains with respect to the springs' elastic constants (case $k_c k_{pn} < 1$)

which gives the condition for choosing the elastic constants k_{es} and k_{ea} of the (18) and (22) springs, in order to ensure the stability, as shown in figure 5.
Condition (54) being accomplished, it results that

$$1 - \frac{k_{px}k_{py}}{k_{AB}\left(k_{pic} + k_{Qx}\right)} > k_c k_{pn} > 0\,, \tag{56}$$

which means that the co-efficient of τ_p and τ_M in (53) are both positive, so this condition is always accomplished.
Consequently, the stability condition for the system is (55) and the stability domains are shown in figure 5. One can also observe that, if the fuel pump actuator's spring is missing, which means that $k_{ea} = 0$, the minimum value for the differential pressure sensor's spring is given by

$$\left(k_{es}\right)_{\min} = \frac{S_{sv}\, Q_{p0}\left(\gamma + 1\right)^2}{\left(\gamma - 1\right)\left(1 - k_c k_{pn}\right)\left(\mu_s b_s \gamma x_0 - \frac{\pi}{4}\mu_d d_d^2 \sqrt{\gamma}\right)}\,, \tag{57}$$

corresponding to the point A, on the ordinates axis, in figure 5.

Case b) $k_c k_{pn} \geq 1$

The condition (54) offers, in this case, an expression similar to (55) and the stability domains as figure 6 shows. One can observe that the unstable domain corresponds to the interval of very small values of the spring's constants, which means that the usual values k_{es} and k_{ea} are in the stable domain.
The condition (53) becomes

$$\tau_M\left[1 - \frac{k_{px}k_{py}}{k_{AB}\left(k_{pic} + k_{Qx}\right)}\right] > \tau_p\left(k_c k_{pn} - 1\right), \tag{53'}$$

which gives

$$\tau_p < \frac{1 - \dfrac{k_{px}k_{py}}{k_{AB}\left(k_{pic} + k_{Qx}\right)}}{\left(k_c k_{pn} - 1\right)}\tau_M\,, \tag{58}$$

or, if one considers the expressions (24) and (39), it becomes, as generic expression, $\tau_p < \frac{f_\tau}{g_\tau}\tau_M$, where

$$f_\tau = \mu_s b_s\left[k_{ea} y_0 + S_A(\gamma - 1)x_0\right]S_{sv}\left(\gamma + 1\right)^2 Q_{p0}\,,$$

$$g_\tau = x_0 y_0\left(\mu_s b_s \gamma x_0 - \frac{\pi}{4}\mu_d d_d^2\sqrt{\gamma}\right)(\gamma - 1)\left[k_{es}S_A(\gamma - 1)Q_{p0} + \mu_s b_s S_{sv} y_0 k_{ea}\left(\gamma + 1\right)\right]. \tag{59}$$

If one uses the annotations

$$a = k_c k_{pn} - 1,\; b = \frac{k_{px}k_{py}}{k_{AB}\left(k_{pic} + k_{Qx}\right)}\,, \tag{60}$$

the condition (58) becomes

$$\tau_p < \frac{1 - b}{a}\tau_M\,, \tag{61}$$

which represents a semi-plan in a co-ordinate system $\left(\tau_M, \tau_p\right)$, as figure 7 shows.

Meanwhile, the characteristic polynomial can be expressed, using the annotations (60), as

$$\tau_p \tau_M s^2 + \left[(1 - b)\tau_M - a\tau_p\right]s - (a + b)\,. \tag{62}$$

The condition for the non-periodic stability is that the above polynomial's roots are real and negative, which means

$$\left[(1 - b)\tau_M - a\tau_p\right]^2 + 4\tau_p\tau_M(a + b) > 0\,, \tag{63}$$

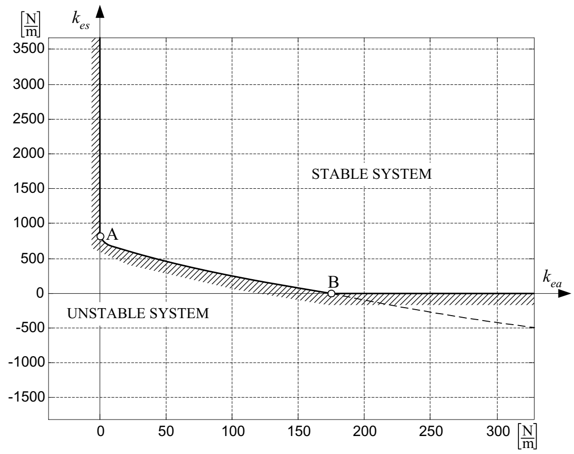

Figure 6: System's stability domains with respect to the springs' elastic constants (case $k_c k_{pn} \geq 1$)

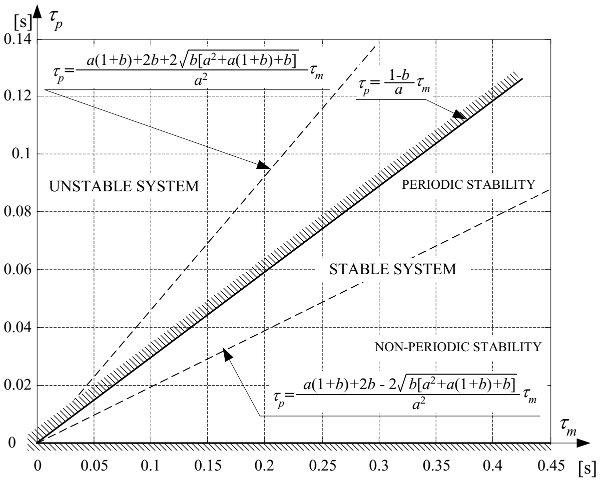

Figure 7: System's stability domains with respect to the time constants τ_M , τ_p (case $k_c k_{pn} < 1$)

$$\frac{\lfloor (1-b)\tau_M - a\tau_p \rfloor}{\tau_p \tau_M} < 0 . \tag{64}$$

The condition (64) is accomplished, being the same as (53), so (63) remains the unique condition for non-periodic stability, which leads to

$$\frac{\tau_p}{\tau_M} < \frac{1}{a^2}\left\{a(1+b)+2b-\sqrt{b\left[a^2+a(1+b)+b\right]}\right\}, \tag{65}$$

$$\frac{\tau_p}{\tau_M} > \frac{1}{a^2}\left\{a(1+b)+2b+\sqrt{b\left[a^2+a(1+b)+b\right]}\right\}. \tag{66}$$

The above presented inequalities represent 2 semi-planes, as figure 7 shows. One can observe that the line $\tau_p = \frac{1}{a^2}\left\{a(1+b)+2b+\sqrt{b\left[a^2+a(1+b)+b\right]}\right\}\tau_M$ is developed in the unstable domain. The other line, $\tau_p = \frac{1}{a^2}\left\{a(1+b)+2b-\sqrt{b\left[a^2+a(1+b)+b\right]}\right\}\tau_M$, belongs to the stable domain and represents the border between the periodic and the non-periodic stable domain.

5. ON SYSTEM'S QUALITY

As the transfer function form shows, the system is a static one, being affected by static error.

One has studied/simulated a controller serving on a single spool jet engine (VK-1 type), from the point of view of the step response, which means the system's dynamic behavior for a step input of the dosage valve's lever's angle θ.

According to figure 8, for a step input of the throttle's position α, as well as of the lever's angle θ, the differential pressure $p_r = p_C - p_i$ has an initial rapid lowering, because of the initial dosage valve's step opening, which leads to a diminution of the fuel's pressure p_C in the pump's chamber; meanwhile, the fuel's flow rate through the dosage valve grows. The differential pressure's recovery is non-periodic, as the curve in figure 8 shows.

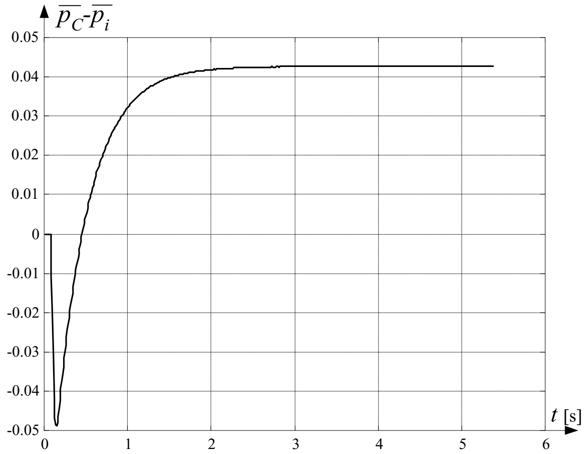

Figure 8: System's differential pressure's $p_r = p_C - p_i$ step response

Theoretically, the differential pressure's re-establishing must be made to the same value as before the step input, but the system is a static-one and it's affected by a static error, so the new value is, in this case, higher than the initial one, the error being 4.2%. The engine's speed has a different dynamic behavior, depending on the $k_c k_{pn}$ particular value.

One has performed simulations for a VK-1-type single spool jet engine, studying three of its operating regimes: a) full acceleration (from idle to maximum, that means from $0.4 \times n_{\max}$ to $n_{\max}$); b) intermediate acceleration (from $0.65 \times n_{\max}$ to $n_{\max}$); c) cruise acceleration (from $0.85 \times n_{\max}$ to $n_{\max}$).

If $k_c k_{pn} < 1$, so the engine is a stable system, the dynamic behavior of its rotation speed n is shown in figure 9. One can observe that, for any studied

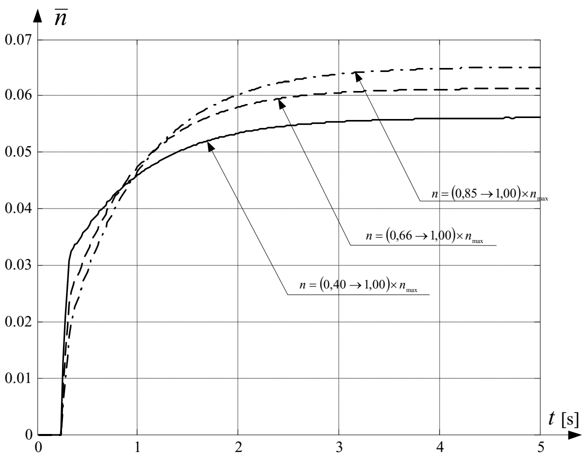

Figure 9: System's speed n step response $\left(k_c k_{pn} < 1\right)$

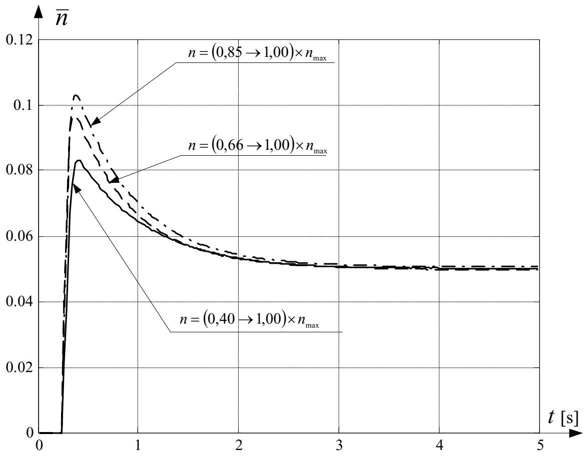

Figure 10: System's speed *n* step response $(k_c k_{pn} \geq 1)$

regime, the speed *n*, after an initial rapid growth, is an asymptotic stable parameter, but with static error. The initial growing is maxim for the full acceleration and minimum for the cruise acceleration, but the static error behaves itself in opposite sense, being minimum for the full acceleration.

If $k_c k_{pn} \geq 1$, the dynamic behavior of its rotation speed *n* is shown in figure 10. Even in this case, after an initial rapid growth, the speed is an asymptotic stable parameter, but with small static error. The initial growth is higher than the stabilization value, as higher as the acceleration is more intense. The static error is nearly constant, being around 4.5%.

6. CONCLUSION

One has studied a speed controller for a single spool jet engine, based on the control of the fuel pump's differential pressure's control. System's non–linear, linearised and non-dimensional mathematical models were presented, as well as the block diagrams and the transfer function.

After performing the stability studies, based on algebraic criteria, some important conclusions could be drawn.

If the couple engine-fuel pump is a stable connection, whole system's stability can be assured by choosing properly the actuator's and the pressure's sensor's spring, from their elastic constant's values k_{ea}, k_{es} point of view.

Otherwise, one must choose properly the time constant's value τ_p for the actuator, according to the jet engine's time constant τ_m. Therefore, in order to ensure the stability, the actuator's time constant must be at most third part of the engine's time constant $\tau_p \leq \frac{\tau_M}{3}$; for the non-periodic stability, the condition is more restrictive, being around $\tau_p \leq \frac{\tau_M}{4}$. The bigger is the $k_c k_{pn}$ value, the smaller must be the actuator's time constant. The τ_p value can be chosen, [see 7,8], by an appropriate choosing of its drossel's diameters as well as its geometric and functional parameters (S_A, k_{ea}, etc).

For an engine VK-1-type, who is a stable system, having $k_c k_{pn} < 1$, the studied rotation speed's control system assures the non-periodic stability, engine's speed *n* being an asymptotic stable parameter. Even if, hypothetically, the studied engine-fuel pump connection would become an unstable system, the rotation speed controller could assure the stable behavior.

References

[1] Abraham, R. H. *Complex dynamical systems,* Aerial Press, Santa Cruz, California, 1986.

[2] Lungu, R. *Flight apparatus automation,* Publisher "Universitaria", Craiova, 2000.

[3] Mattingly, J. D. *Elements of gas turbine propulsion.* McGraw-Hill, New York, 1996.

[4] Stevens, B.L., Lewis, E. *Aircraft control and simulation,* John Willey Inc. N. York, 1992.

[5] Stoenciu, D. *Aircraft engine automation. Aircraft engines as controlled objects,* Publisher of Military Technical Academy, Bucharest, 1977.

[6] Stoenciu, D. *Aircraft engine automation. Album with automation schemes,* Publisher of Military Technical Academy, Bucharest, 1977.

[7] Stoicescu, M., Rotaru, C. *Turbo-jet engines. Characteristics and control methods,* Publisher of Military Technical Academy, Bucharest, 1999.

[8] Tudosie, A. *Aerospace propulsion systems automation*, Inprint of University of Craiova, 2005.